Materials Transactions, Vol. 50, No. 8 (2009) pp. 2092 to 2097

EXPRESS REGULAR ARTICLE

Synthesis, Characterization and Effect of pH Variation on Zinc Oxide Nanostructures

Rizwan Wahab, Young-Soon Kim and Hyung-Shik Shin*

Energy Materials & Surface Science Laboratory, Solar Energy Research Center, School of Chemical Engineering, Chonbuk National University, 664-14 Deokjin-dong, Deokjin-gu, Jeonju-si, Jeonbuk 561-756, Korea

Here we present a systematic study on the morphological deviation of ZnO nanostructure (from sheets to micro-flowers) by varying pH of the solution via precipitation method. In this regard, zinc nitrate hexa-hydrate, NaOH and hydroxylamine hydrochloride ($NH_2OH{\cdot}HCl$) were used. The solution of all three compounds was refluxed at a very low temperature (60°C) for short time (20 min). The solution pH was calibrated from 6 to 12 by the controlled addition of NaOH and HCl. We have observed from FESEM (field emission scanning electron microscopy) that the morphology of ZnO microballs composed with thin sheets markedly varies from sheet (at pH = 6) to micro-flower composed with sheets of zinc oxide (pH = 10–12). Further the morphology and crystallinity were also studied by the TEM (transmission electron microscopy) and HR-TEM (High resolution transmission electron microscopy) and it's clearly consistent with the FESEM observations. The FTIR spectroscopic measurement also confirms the compositional analysis of ZnO and it comes in the range of 475 to 424 cm^{-1} which is a standard peak of ZnO. In addition to this, the amount of H^+ and OH^- ions are found a key to control the structure of studied material and discussed in the growth mechanism. [doi:10.2320/matertrans.M2009099]

(Received April 1, 2009; Accepted June 1, 2009; Published July 25, 2009)

Keywords: *ZnO, hydroxylamine hydrochloride, nanostructures, pH variation*

1. Introduction

The semiconductor zinc oxide (ZnO) is a promising material because of its unique properties and wide range of advanced technological applications.[1)] Zinc oxide (ZnO) has received considerable attention because it has optical, semiconducting, piezoelectric, magnetic and gas sensing properties. ZnO nanostructures exhibit interesting properties including, high exciton binding energy (60 meV), high chemical stability, high catalytic efficiency, strong adsorption ability and low growth temperature makes it an excellent candidate for room temperature UV lasing application. These days, much emphasis is given on the application of ZnO is in biosensing because of its high isoelectric point (9.5), biocompatibility, and fast electron transfer kinetics. Such features support nanostructured synthesis and use of this exciting material for such novel unexplored applications.[2–8)]

Several deposition technique have been employed for the synthesis of zinc oxide nanostructures (nanowires, nanobelts, nanobridges, nanonails, nanoribbons, nanorods, nanotubes, and whiskers) such as physical evaporation, hydrothermal, chemical vapor deposition, cyclic feeding chemical vapor deposition, thermal evaporation, metal organic chemical vapour deposition (MOCVD), spray pyrolysis, ion beam assisted deposition, laser-ablation, sputter deposition, template assisted growth and solution method etc.[9–19)] In addition to these techniques, precipitation/solution method is a prominent and most effective process because it offers many advantages with excellent and control over stoichiometry, compositional modification, microstructure control using capping molecules, controlled doping, with inexpensive equipments. As we know that the properties of zinc oxide strongly depends on the synthesis method and conditions during processing. The growth habit of zinc oxide is greatly affected by the external conditions such as reaction temperature, reaction concentration, pH value of the solution.[20)] It is well known that the morphology of the precipitation/solution synthesized metal-oxides strongly depend on the amount of H^+ or OH^- ions in the sol that effectively determines the polymerization of the metal–oxygen bonds. Precursor solution pH variation affects the hydrolysis and condensation behavior of the solution during gel formation, and hence influences the morphology. Literature survey indicates that the effect of pH on the morphology/properties of ZnO is rare being an important factor to determine the quality. The pH of solution appears to be critical parameter for the phase formation, particles size and morphology of the structure during solution method. Several researchers have been synthesized zinc oxide nanostructures by using various chemical precursors and different processing methods such as Li *et al.*, presented the preparation of ZnO nanostructures on SiO_2-buffered Si substrates. The solution pH value was varied to synthesize rod and platelet using the sol–gel method.[21)] Pal *et al.*, presented the synthesis of various types of zinc oxide nanostructures by using ethylenediamine, zinc acetate di-hydrate and sodium hydroxide and water at two different pH values by the hydrothermal method.[22)] Hochepied *et al.*, obtained the pompom like zinc oxide nanostructures by using zinc nitrate hexahydrate and ammonia. The solution was heated in a thermostat reactor and chacked pH evolution.[23)] Bai *et al.*, presented the rose like zinc oxide nanostructures by using $ZnCl_2$ and ammonia (25%) synthesized through a hydrothermal decomposition method on a copper plate substrate.[24)]

In all the results reported above, the nanostructures were grown either at higher temperature or they need, sophisticated instruments, expensive chemicals and complex reaction procedure for the growth of zinc oxide nanostructures. In this paper we report a systematic study on the morphological variation of ZnO nanostructures by controlling the pH (6–12), of the solution of zinc nitrate hexa-hydrate ($Zn(NO_3)_2{\cdot}6H_2O$), hydroxylamine hydrochloride ($NH_2OH{\cdot}HCl$) and

*Corresponding author, E-mail: hsshin@chonbuk.ac.kr

sodium hydroxide (NaOH) at a very low temperature (60°C) and in a very short refluxing (20 min) time. To the best of our knowledge the use of hydroxylamine hydrochloride for the synthesis of disk to micro flower formation by the calibration of pH is presented first time and such type of report is not available in the literature. In addition to this, on the basis of morphological and chemical observations a possible growth mechanism is also proposed.

2. Experimental

2.1 Material synthesis

Synthesis of zinc oxide nanostructures were carried out by only the calibration of pH values using zinc nitrate hexa-hydrate ($Zn(NO_3)_2{\cdot}6H_2O$), hydroxylamine ($NH_2OH{\cdot}HCl$) hydrochloride and sodium hydroxide (NaOH) as precursors. The experimental condition is characterized in four steps as follows:

Step-1: (Mixing of precoursors): In first step 0.3 mole concentration of zinc nitrate hexa-hydrate ($Zn(NO_3)_2{\cdot}6H_2O$), 0.1 mole hydroxylamine hydrochloride and 3 mole sodium hydroxide were dissolved in 100 ml distilled water (DW) and stirred the solution for 30 min.

Step-2: (pH observation): After mixing of zinc nitrate hexa-hydrate ($Zn(NO_3)_2{\cdot}6H_2O$), hydroxylamine hydrochloride and sodium hydroxide a white colored solution was observed in beaker. The pH value of this solution was measured by expandable ion analyzer EA 940 (Orion, UK) and it was observed at this time 12.9.

Step-3: (Desired pH calibration): In third step, the pH value of the solution was adjusted to the desired value (from 6 to 12) by using 1 mole NaOH and 1 mole HCl solution (each in 100 ml deionized distilled water) and was added drop by drop.

Step-4: (Refluxing of desired pH solution): In fourth step, the modified solution was transferred in a three-necked refluxing pot and refluxed at 60°C for 20 min.[25,26] The refluxing temperature was measured by k-type thermocouple and controlled by using a PID controller. While refluxing, pH of the solution was neither measured nor controlled. After refluxing, the white precipitate was washed with methanol several times, dried at room temperature and was examined in terms of their structural and chemical properties.

2.2 Characterization

Samples were observed using field emission scanning electron microscopy (FESEM) and transmission electron microscopy (TEM) for the morphological and detailed structural information. For SEM observation, powder was uniformly sprayed on a carbon tape pasted on the specimen holder. In order to avoid charging while observation, the powder was coated with thin OsO_4 (~10 nm) layer. For the transmission electron microscopic (TEM) measurement, powder was sonicated in ethanol for 10 min there by dipping copper grid in the solution and drying at room temperature. The crystallinity and crystal phases were determined by X-ray powder diffractometer (XRD) with CuKα radiation ($\lambda = 0.154178$ nm) at the Bragg angle ranging from 30° to 65°. The composition of the synthesized ZnO nanostructures were characterized by the Fourier transform infrared (FTIR) spectroscopy in the range of 4000–400 cm^{-1}. In addition to this, the optical properties of the samples were also studied by the UV-visible (UV-vis) absorption double beam spectrophotometer with a deuterium and tungsten iodine lamp in the range from 300–500 nm at room temperature. All the powder samples were dispersed in the de-ionized water and sonicate for 10 min for the complete dispersion of the samples.

3. Results and Discussion

3.1 X-Ray diffraction analysis (XRD)

Figure 1 shows the X-ray diffraction pattern of sheet to micro balls like zinc oxide nanostructures as a function of increasing pH values. All the diffraction peaks in the pattern is well matched with the available Joint Committee on Powder Diffraction Standards for bulk ZnO (JCPDS 36-1451) and are indexed as the hexagonal zinc oxide with lattice constants $a = 0.3249$ and $c = 0.5206$ nm. Additionally, higher intensity and narrower spectral width of ZnO peaks in the spectrum affirmed that the obtained products have good crystallinity.

3.2 Field emission scanning electron microscopy (FESEM)

Figure 2 shows the morphological variation with solution pH. An organized change occurs in the structure from rounded disk like nanostructure to a micro-flower composed with nano sheets. Figure 2(a) shows the high magnification image of zinc oxide with sheet/plate like structure when synthesized at the solution pH = 6. Figure 2(b) presents the high magnification image of synthesized zinc oxide nanostructures at the neutral solution pH = 7. Thick sheet like structure is evident accumulated in one position. A deviation from the sheet-like structure to sort of aligned plate and rod like structure is evident at pH (= 8). Further increase in the solution pH (= 9) results in total conversion of rounded individual sheet to microflowers like accumulated with several sheets in one flower can be seen in Fig. 2(d). When the pH value of the solution increased to pH = 10, only bunches of microflowers was observed with two dimensional flat surface shape (Fig. 3(a) and (b)). Figure 3(c) and 3(d) shows the low and high magnification images of synthesized

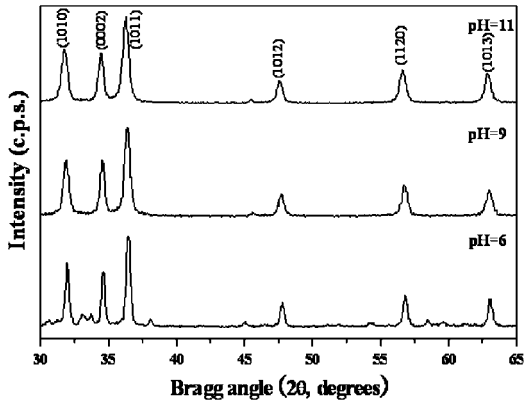

Fig. 1 Typical X-ray diffraction pattern of Synthesized zinc oxide nanostructures at different pH values.

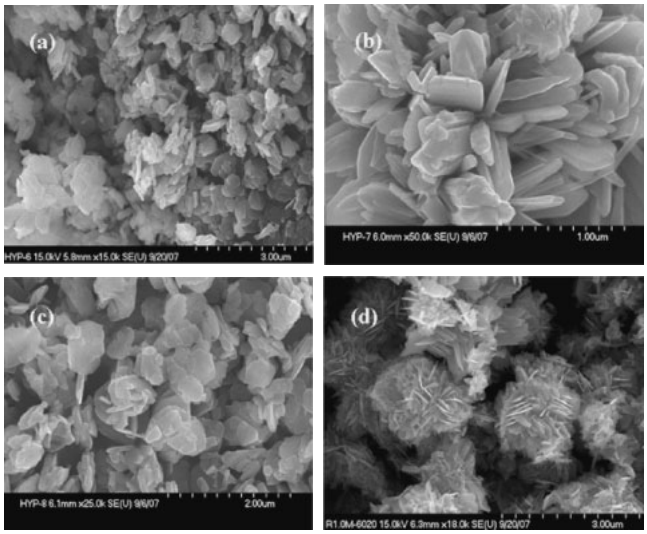

Fig. 2 FESEM images of spherical shaped disk like grown zinc oxide nanostructures (a) at pH 6, (b) at pH 7, (c) at pH 8, (d) at pH 9.

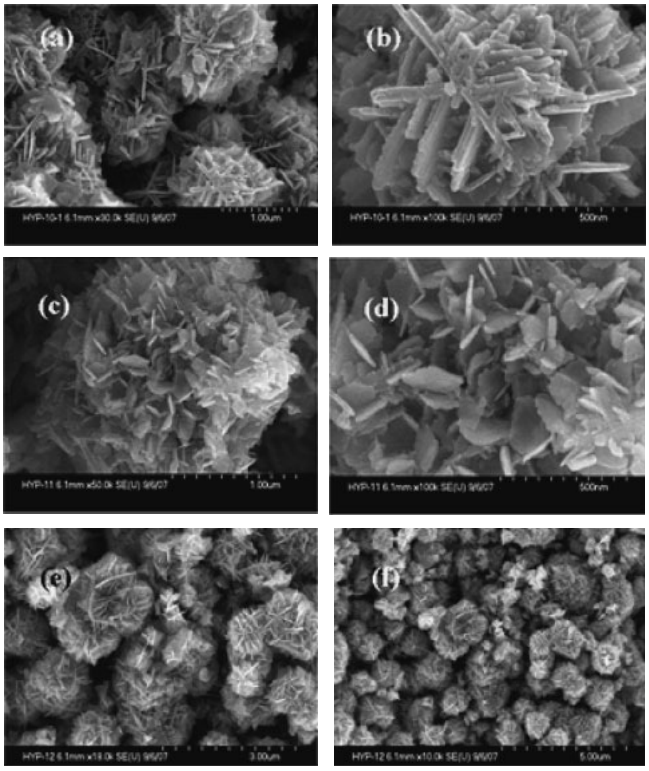

Fig. 3 Low and high magnification FESEM images of micro-flower composed with sheets of grown zinc oxide nanostructures (a–b) at pH 10, (c–d) at pH 11, (e–f) at pH 12.

zinc oxide nanostructures at pH = 11, where nanosheets are seen forming a flower like structure. Synthesis at pH = 12, results in a complete flower like morphology composed to flat plate like two dimensional sheets (Fig. 3(e) and (f)).

3.3 Transmission electron microscopy (TEM)

Further the morphological characterization was also carried out by the transmission electron microscopy (TEM) and high resolution TEM (HR-TEM) equipped with the selected area electron diffraction (SAED) pattern.

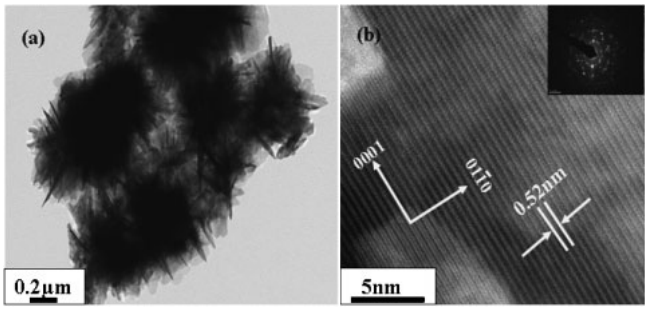

Fig. 4 (a) Low magnification TEM image of the grown ZnO micro flower shaped morphology and their corresponding SAED pattern (inset), (b) HRTEM image shows the difference between two lattice fringes, which is about 0.52 nm. The corresponding SAED pattern (inset) consistent with the HRTEM observations and indicate the crystallinity of the synthesized products.

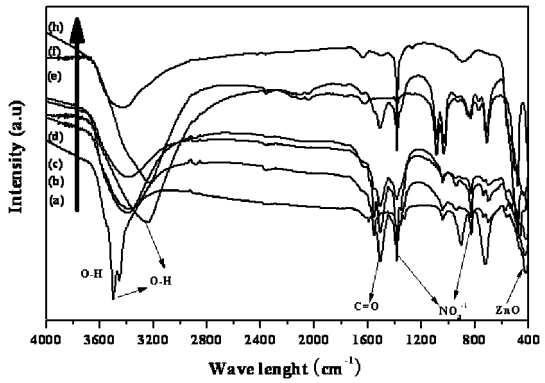

Fig. 5 Typical FTIR spectra of grown product at different pH conditions from 6 to 12 (a)–(h).

Figure 4(a) shows the low magnification TEM image of ZnO micro-flower grown at pH = 11. The TEM image is clearly consistent with the FESEM observations. The corresponding SAED pattern obtained from the sheets confirms that the synthesized products are crystalline and grew along the [0001] direction (shown as inset in Fig. 4(b)). Figure 4(b) shows the high resolution TEM (HRTEM) image of a nanosheets or flowers leaf. The lattice fringes between two adjacent plane is about 0.52 nm, which is equal to the lattice constant of the ZnO which further indicate that the synthesized structure have a wurtzite phase and are preferentially grown. The corresponding SAED pattern (inset in Fig. 4(b)) is consistent with the HR-TEM observation.

3.4 FTIR measurement

Figure 5 show the compositional analysis of as grown zinc nanostructures at different pH (from 6 to 12) was carried out by the FTIR measurement at room temperature in the acquired range of 4000–400 cm^{-1}. The bands at 3200–3600 cm^{-1} correspond to O–H mode of vibration, here we can easily see that the position of O-H peaks changes from sharp (pH = 6) to broad peaks (pH = 7–12), which indicates that in acidic condition (at pH = 6) grown sheets was undeveloped (Fig. 2(a) and (b)) but as the pH value moves to neutral (pH = 7) and in basic region (pH = 8–12) sheets

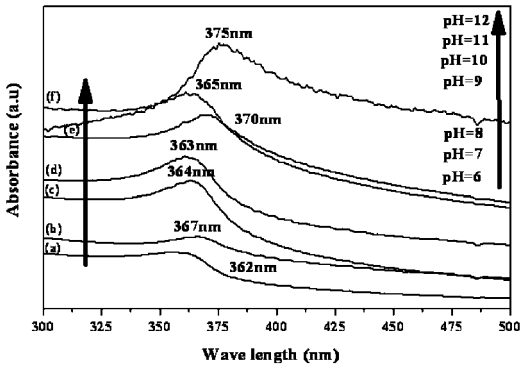

Fig. 6 Typical UV-vis spectra of different shaped zinc oxide nanostructures at different pH conditions (pH 6 to 12).

were changes in to micro-flowers. The movement of O-H peak plays an important role in the structure formation and it is very clear Form FESEM and TEM images. The strong asymmetric stretching mode of vibration of C=O was observed between 1566–1547 cm^{-1}. As the pH value of zinc nitrate hexa hydrate ($Zn(NO_3)_2{\cdot}6H_2O$) and hydroxylamine hydrochloride ($NH_2OH{\cdot}HCl$) solution increases by the addition alkali sodium hydroxide, the vibration peak of C=O was shifted up and down which is due to the structural change in the morphology as observed from the FESEM images (Figs. 2 and 3) and the symmetric stretching occurs between 1385–821 cm^{-1} indicates the vibration of $NO_3{}^{-1}$ ions.[27,28] The standard peak of zinc oxide nanostructures was appeared in the range 475–424 cm^{-1}. From Fig. 5 we can easily see that as the solution pH increases the vibration band of zinc oxide decreases from 475 to 424 cm^{-1} wave number. This change indicates the changes in morphology of zinc oxide, analogous to FESEM and TEM observations.

3.5 Optical characterization (UV-vis Spectroscopy)

The optical properties of as-grown zinc oxide nanostructures synthesized at various pH conditions were examined by UV-vis spectroscopy at room-temperature and demonstrated in Fig. 6. A broad peak has been found in all the pH values in the range of 362–375 nm, which is a characteristic/standard peak of wurtzite hexagonal phase ZnO, demonstrating that the synthesized products are pure ZnO.[29,30] The obtained band gap of our synthesized nanostructures (~3.42 eV) at room-temperature UV-vis spectra is well matched with the standard bulk ZnO (~3.37 eV).[30] Due to the presence of a broad peak in the obtained UV-vis spectra, one can easily conclude that the grown ZnO nanostructures exhibited good optical properties and containing wurtzite hexagonal phase.

3.6 Possible growth mechanism and effect of pH on the zinc oxide nanostructures

On the basis of microscopic results, we can easily predict the possible plausible growth mechanism for the formation of micro-flowers shaped ZnO structures by variation of solution pH. The growth of micro flowers comprises of two steps: nucleation or formation of spherical molecules and its growth into flowers shaped structure. When an aqueous solution of zinc salts ($Zn(Ac)_2{\cdot}2H_2O$), $Zn(NO_3)_2{\cdot}6H_2O$, $ZnCO_3$ and $ZnCl_2$ etc.) reacts, compounds with low solubility precipitate out of the solutions. It is well known to control the structural morphology of the zinc oxide nanostructures by employing various salts and controlling processing parameters such as temperature, amount of the salt and the pH value of the solution.

In order to understand the effect of pH on the zinc oxide nanostructures, here we have systematically adjusted the pH values from 6 to 12 by using alkali sodium hydroxide (1 Mole) and hydrochloric acid (1 Mole) solution dilution in the precursor solution and refluxed each solution at 60°C in a tri-necked refluxing pot for only 20 min. As per the microscopic observations (FESEM and TEM), it is found that the morphology markedly depends on the pH of the solution. When an aqueous zinc nitrate hexahydrate ($Zn(NO_3)_2{\cdot}6H_2O$) and hydroxylamine hydrochloride ($NH_2OH{\cdot}HCl$) were mixed, no precipitate was observed But after the incorporation of NaOH solution a white precipitate was observed for few seconds. At this time solution pH was also maintained by using sodium hydroxide and hydrochloric acid. After getting desired pH, the solution was further refluxed for the complete growth of nanostructures. In this case, when NaOH was added to the solution of zinc nitrate hexahydrate ($Zn(NO_3)_2{\cdot}6H_2O$) and hydroxylamine hydrochloride ($NH_2OH{\cdot}HCl$). The precipitates of $Zn(OH)_2$ were dissociated into Zn^{2+} and OH^- ions in the presence of water and thermal energy (i.e. while refluxing). It is expected when the concentration of these Zn^{2+} and OH^- ions exceeds the critical value, the precipitation of ZnO nuclei starts. One can call this process as the initial nucleation process for the formation of ZnO. The changes in Zn^{2+} and OH^- ions can be correlated to the increase in thermal energy of the system. At present it is difficult to mention here about the corresponding quantitative changes in the OH^- concentration since the pH of the solution was not measured/controlled while synthesis. As the reaction temperature increases the dissociation of the zinc complex ($Zn(OH)_2$) and leads to the controlled release of free zinc ions (Zn^{2+}) and hydroxide ions. The following reaction occurs immediately:

$$Zn(OH)_2 \rightarrow Zn^{2+} + 2OH^- \quad (1)$$

$$Zn^{2+} + H_2O \rightarrow ZnO + 2H^+ \quad (2)$$

$$ZnO + H_2O \rightarrow ZnO_2{}^{2-} + 2H^+ \quad (3)$$

It is expected to contain small spherical molecules of zinc hydroxide ($Zn(OH)_2$) changes into zinc (Zn^{2+}) ions and when this ions react with the water molecule it forms zinc oxide (ZnO as eqs. (1)–(3)) hydroxyl ions as schemated in Fig. 7(a)–(b). The zinc oxide (ZnO) molecule grows slowly due to the energy acquired from stirring, (schemated as Fig. 7(c)–(d)) and forms a small spherical disk like structures by refluxing of this solution.[31] Solution grown zinc oxide nano structures produces in acidic medium (pH = 6) consisting spherical sheet like structures and when these sheets are accumulated, it forms a leaf (Fig. 7(e)) like structure. In acidic medium solution's concentration of H^+ ions increases more and more and preferably reacted with hydroxyl ions (OH^-) at the surface of sheets of zinc oxide nanostructures and it inhibits growth along [0001] direction. The increases in pH value causes by the consuming of H^+ ions during the growth of spherical sheets and it leads to the

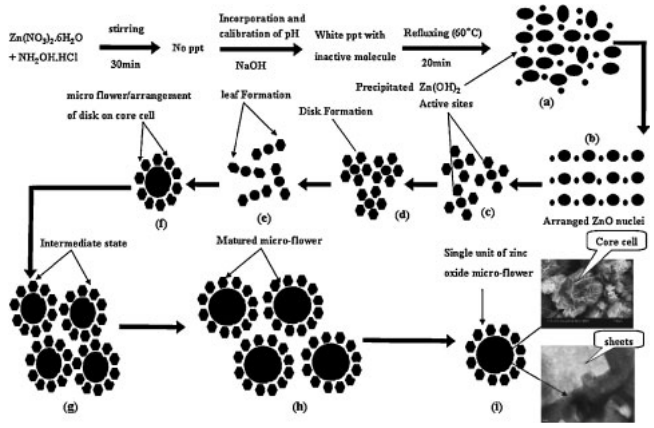

Fig. 7 Possible growth mechanism of spherical shaped zinc oxide nanosheets to micro-flower by varying pH from 6–12.

favorable conditions for the growth of spherical sheets at the boundaries between the platelets.[21] With refluxing, conversion form $Zn(OH)_2$ to ZnO occurs[27] However, the increasing pH influences the structure of ZnO as the amount of H^+ or OH^- ion changes. The nanostructures of zinc oxide directly affected by the influence of pH of the solution and its is very clear from the FTIR peaks and FESEM images. The small sheets grows and changes in to micro-flowers. It is expected that the effective density of H^+ ions will be low at higher pH than that of at lower pH values. Higher amount of H^+ ions will inhibits the hydrolysis and condensation processes, leading to the smaller aggregates at the end of polycondensation process, as schemated in Figs. 7(a) to (e). When the acidic solution changes to the neutral solution ($pH = 7$), the number of H^+ (hydrogen) ions decreases in the solution and it will reacts with the OH^- ion equally on the surface of grown sheets. The neutral solution not much affected and has very littlie influence at the interfaces of zinc oxide crystals that's why it grows the [0001] direction. In basic solutions (above $pH = 7$), the number of OH^- (hydroxyl) ions in higher amount and are strongly attracted by the positively charged, Zn-terminated, surfaces. A strong Zn-O bond was formed, which promotes a Zn bond in the structure.[21] In addition to this, the effective OH^- ions density increases as the pH of the solution increases by the addition of 1 mole NaOH Solution. Therefore, the reaction would be governed by the hydroxyl ions (OH^-). Although, the initial growth leads to the formation of plate like structure (sort of linear chain formation, Figs. 2(a) and (b) but due to high OH^- ions, it results in cyclization, since the probability of intermolecule reaction is higher than intramolecule reaction.[32] At higher pH values, hydrolysis/condensation is uncontrolled and unselective which leads to a highly branched sheets with arranged in a flower like structures ($pH = 9$) (Fig. 7(f)). At the same time, it will also generate larger interconnected particles/structure. At pH 10 the sheets are not fully developed but as the OH^- concentration ($pH = 11$ and 12) increases by the addition of 1 mole NaOH solution. The grown sheets are arranged in spherical flower shaped morphology. FESEM and TEM images (Figs. 3(e) and 3(f)) clearly consistent with the schemated as Figs. 7(g) to (i).

4. Conclusions

A systematic study of pH variation by using zinc nitrate hexahydrate ($Zn(NO_3)_2 \cdot 6H_2O$), hydroxylamine hydrochloride ($NH_2OH \cdot HCl$) and sodium hydroxide (NaOH) was presented and it's was found that the morphology of ZnO nanostructures depends on the pH of the precursor solution. Small spherical sheets to micro-flower composed with sheets like structure were changes with increased pH values from 6 to 12. On the basis of microscopic (FESEM and TEM) studies we can easily concluded that the size/morphology of the structure can be tailored by pH variation. In addition to this, the optical properties (UV-vis spectroscopy) of the grown samples at different conditions were also shown good optical properties as compared to the bulk ZnO. On the other hand, the crystallinity and compositional analysis indicated that the solution pH does not affect much on the quality of the material as observed from X-ray diffraction pattern and FTIR spectroscopy.

Acknowledgement

Support from KOSEF research grant no. R01-2007-000-20810-0 is fully acknowledged. We also would like to acknowledge KBSI, Republic of Korea, Jeonju branch, for access to their FESEM Facility and Mr. Kang Jong-Gyun at the Center for University-Wide Research Facilities, Chonbuk National University, for his cooperation in TEM observations.

REFERENCES

1) P. Yang, H. Yan, S. Mao, R. Russo, J. Johnson, R. Saykally, N. Morris, J. Pham, R. He and H.-J. Choi: Adv. Funct. Mater. **12** (2002) 323–331.
2) H. Cao, J. Y. Xu, E. W. Seelig and R. P. H. Chang: Appl. Phys. Lett. **76** (2000) 2997–2999.
3) S. W. Chung, J.-Y. Yu and J. R. Health: Appl. Phys. Lett. **76** (2000) 2068–2070.
4) Y. Chen, D. M. Bangall, H. Koh, K. Park, K. Hiraga, Z. Zhu and T. Yao: J. Appl. Phys. **84** (1998) 3912–3918.
5) B. J. Jin, S. H. Bae, S. Y. Lee and S. Im: Mater. Sci. Eng. B **71** (2000) 301–305.
6) G. S. Lieri, S. Groppelli, P. Nelli, A. Tintinelli and G. Giunta: Sensor. Actuat. B **25** (1995) 588–590.
7) J. A. Rodriguez, T. Jirsak, J. Dvorak, S. Sambasivan and D. J. Fischer: J. Phys. Chem. B **104** (2000) 319–328.
8) Z. L. Wang: Mater. Today **7** (2004) 26–33.
9) A. Umar, S. Lee, Y. S. Lee, K. S. Nahm and Y. B. Hahn: J. Cryst. Growth **277** (2005) 479–484.
10) J. Y. Park, H. Oh, J.-J. Kim and S. S. Kim: J. Cryst. Growth **287** (2006) 145–148.
11) Y. Li, G. W. Meng and L. D. Zhang: Appl. Phys. Lett. **76** (2000) 2011–2013.
12) S. Y. Li, C. Y. Lee and T. Y. Tseng: J. Cryst. Growth **247** (2003) 357–362.
13) W. Z. Pan, R. Z. Dai and Z. L. Wang: Science **291** (2001) 1947–1949.
14) J. Y. Lao, J. Y. Huang, D. Z. Wang and Z. F. Ren: Nano Lett. **3** (2003) 235–238.
15) S. A. Studenikin, N. Golego and M. Cocivera: J. Appl. Phys. **84** (1998) 2287–2294.
16) Y. J. Xing, Z. H. Xi, Z. Q. Xue, X. D. Zhang, J. H. Song, R. M. Wang, J. Xu, Y. Song, L. Zhang and D. P. Yu: Appl. Phys. Lett. **83** (2003) 1689–1691.
17) J. Q. Hu and Y. Bando: Appl. Phys. Lett. **82** (2003) 1401–1403.

18) H. Zahang, D. Yang, D. Li, X. Ma, S. Li and D. Que: J. Cryst. Growth Design **5** (2005) 547–550.
19) K. Haga, F. Katahira and H. Watanabe: Thin Solid Films **343** (1999) 145–147.
20) T. Sekiguchi, K. Haga and K. Inaba: J. Cryst. Growth **214–215** (2000) 68–71.
21) J. Li, S. Srinivasan, G. N. He, J. Y. Kang, S. T. Wu and F. A. Ponce: J. Cryst. Growth **310** (2008) 599–603.
22) U. Pal, J. G. Serrano, P. Santiago, G. Xiong, K. B. Ucer and R. T. Williams: Opt. Mat. **29** (2006) 65–69.
23) J. F. Hochepied, A. P. A. Oliveira, V. G. Ferreol and J. F. Tranchant: J. Cryst. Growth **283** (2005) 156–162.
24) W. Bai, K. Yu, Q. Zhang, X. Zhu, D. Peng, Z. Zhu, N. Dai and Y. Sun: Phys. E **40** (2008) 822–827.
25) A. Umar, Y. B. Hahn and D. H. Kim: Electrochim. Acta (2009) in press.
26) P. Uthirakumar, Y. S. Lee, E. K. Suh and C. H. Hong: Phys. Lett. A **359** (2006) 223–226.
27) R. Wahab, S. G. Ansari, H. K. Seo, Y. S. Kim, E. K. Suh and H. S. Shin: Solid State Sci. **11** (2009) 439–443.
28) L. Wu, Y. Wu and L. Wei: Phys. E **28** (2005) 76–82.
29) R. Wahab, S. G. Ansari, Y. S. Kim, H. K. Seo, G. S. Kim, G. Khang and H. S. Shin: Mater. Res. Bull. **42** (2007) 1640–1648.
30) R. Wahab, S. G. Ansari, Y. S. Kim, H. K. Seo and H. S. Shin: Appl. Surf. Sci. **253** (2007) 7622–7626.
31) K. S. Suslick: Science **247** (1990) 1439–1445.
32) P. K. Sharma, M. H. Jilavi, V. K. Varadan and H. Schmid: J. Phys. Chem. Solids **63** (2002) 171–177.